Alexander Jöhl, Stephanie Lang, Stefanie Ehrbar, Matthias Guckenberger, Stephan Klöck, Mirko Meboldt and Marianne Schmid Daners*

Modeling and performance evaluation of a robotic treatment couch for tumor tracking

DOI 10.1515/bmt-2015-0187
Received September 29, 2015; accepted February 20, 2016; online first March 25, 2016

Abstract: Tumor motion during radiation therapy increases the irradiation of healthy tissue. However, this problem may be mitigated by moving the patient via the treatment couch such that the tumor motion relative to the beam is minimized. The treatment couch poses limitations to the potential mitigation, thus the performance of the Protura (CIVCO) treatment couch was characterized and numerically modeled. The unknown parameters were identified using chirp signals and verified with one-dimensional tumor tracking. The Protura tracked chirp signals well up to 0.2 Hz in both longitudinal and vertical directions. If only the vertical or only the longitudinal direction was tracked, the Protura tracked well up to 0.3 Hz. However, there was unintentional yet substantial lateral motion in the former case. And during vertical motion, the extension caused rotation of the Protura around the lateral axis. The numerical model matched the Protura up to 0.3 Hz. Even though the Protura was designed for static positioning, it was able to reduce the tumor motion by 69% (median). The correlation coefficient between the tumor motion reductions of the Protura and the model was 0.99. Therefore, the model allows tumor-tracking results of the Protura to be predicted.

Keywords: medical control systems; medical robotics; oncology; tumor motion compensation.

***Corresponding author: Marianne Schmid Daners,** Product Development Group Zurich, Department of Mechanical and Process Engineering, ETH Zurich, CLA G21.1, Tannenstrasse 3, Zurich 8092, Switzerland, Phone: +41 44 632 24 47, E-mail: marischm@ethz.ch
Alexander Jöhl: Product Development Group Zurich, Department of Mechanical and Process Engineering, ETH Zurich, Zurich 8092, Switzerland; and Department of Radiation Oncology, University Hospital Zurich, Zurich 8091, Switzerland
Stephanie Lang, Stefanie Ehrbar, Matthias Guckenberger and Stephan Klöck: Department of Radiation Oncology, University Hospital Zurich, Zurich 8091, Switzerland; and University of Zurich, Zurich 8006, Switzerland
Mirko Meboldt: Product Development Group Zurich, Department of Mechanical and Process Engineering, ETH Zurich, Zurich 8092, Switzerland

Introduction

Along with surgery and chemotherapy, radiation therapy is one of the three main options in cancer treatment. Its efficacy largely depends on the absorbed radiation dose. An increased dose to the tumor leads to a better tumor control. However, at the same time the healthy tissue around the tumor receives a higher dose, which leads to increased side effects. Therefore, a big challenge in radiation therapy is to control the tumor with sufficient dose, while keeping the complication rate for normal tissue reasonably low. There are always uncertainties in the treatment chain in radiation therapy. They lead to the concept of margins, meaning that not only the tumor itself is irradiated but also a margin around the tumor to ensure enough dose to the tumor. The motion of tumors in the thorax and abdomen is one factor contributing to these uncertainties. The patient's respiration causes a time-varying position of thoracic, liver, and adrenal gland tumors. The motion of lung tumors has been reported to have a peak-to-peak amplitude of up to 24 mm [19] or even 38 mm [6]. A liver tumor may move up to 34 mm [18], and the thoracic wall may move up to 14 mm [17]. Therefore, a mitigation of the tumor motion allows the decrease of the margins and, consequently, the reduction of the irradiated healthy tissue.

There are several methods to mitigate respiratory tumor motion [14], 1) respiratory gating monitors the tumor motion, and only if the tumor is in a specific respiration phase, the radiation beam is switched on. This leads to increased time needed for each treatment session. 2) Breath-hold gating means that the patient holds the breath, thereby holding the tumor position. Only then the beam is switched on. This also results in increased treatment time, although the increase might be smaller than for respiratory gating. However, breath-hold may not be feasible for all patients, especially those with reduced lung function. 3) Tumor tracking continuously compensates for tumor motion. This is possible by moving the beam source, modifying the beam, or moving the patient using a robotic treatment couch. These methods are more difficult to implement and

require more technical resources than respiratory gating or breath-hold gating.

Robotic treatment couch tracking can be implemented on conventional, widely available C-arm linear accelerators. Additionally, tumor tracking with a couch leaves the treatment beam undisturbed, which reduces the dosimetric error of the treatment and makes quality assurance easier than with other techniques. The patient is placed on a treatment couch which moves in the opposite direction of the tumor motion to compensate it. The goal is to minimize the patient's tumor motion relative to the radiation beam, which, in turn, allows the margins to be decreased. Thus, the radiation dose to healthy tissue can be decreased, which might ultimately lead to a reduction of side effects, e.g. pneumonitis.

The behavior of the robotic treatment couch is of utmost importance in tumor tracking, as it sets limits on the tumor-tracking performance. A general study in this direction was described in [7], where the authors developed specifications of an ideal treatment couch design for tumor tracking.

In the current study, we assessed the clinically available treatment couch Protura (CIVCO Medical Solutions, Kalona, IA, USA) with respect to its performance in tumor tracking. In addition, we developed and tested a numerical model of the Protura. To our knowledge, no model for the Protura has been developed as yet, although it allows a quick preliminary testing of control strategies for tumor tracking using the Protura. Other treatment couches have been assessed in the literature, for example, the ELEKTA Precise Table (ELEKTA, Stockholm, Sweden) [2, 9], and the HexaPOD (Medical Intelligence GmbH, Schwabmünchen, Germany) [2, 10]. Both couches were modeled in [2] using theory of mechanics and which were numerically simulated with tumor motion signals obtained from real patient data. In [10], the HexaPOD was modeled employing the blackbox approach and chirp signals to obtain parameter identification data. In [9], the ELEKTA Precise Table was modeled with a blackbox approach. A control algorithm was then developed using the model.

In our study, the Protura was modeled using theories of mechanics and of chirp signals. The Protura and the model were set to track the same recorded tumor motion signals and the position of the Protura was measured. Their tracking errors, compared to the case without tracking, were evaluated. The model allows different concepts of treatment couch tumor tracking to be tested and the tracking errors of the Protura to be predicted.

Materials and methods

The Protura was modeled and the performances of the model and the Protura were compared. The tracking error was defined as the Euclidean distance between the tumor center and the planned tumor center. The potential reduction of the tracking error depends on both the accuracy of the knowledge of the tumor motion and the performance of the actuator, namely the treatment couch. This study assumed perfect knowledge of the tumor position relative to the patient position, and only the performance of the treatment couch was considered. The treatment couch investigated was the Protura, which in this case was in use at a clinical linear accelerator. For the preparation of further experiments on real couch tracking with the Protura, a model was developed that allowed preliminary numerical simulations. The model parameters were identified with experiments that were carried out to determine the Protura's performance for tumor tracking. The performance of the Protura was evaluated using the maximum speed and acceleration of the Protura as well as using Bode diagrams.

System description

A schematic overview of the Protura is shown in Figure 1. The patient is placed on the platform and its extension. The latter allows the beam source to be rotated by 360° around the patient. Additionally, the extension is removable from the platform via the platform-extension joint, which is rigid in the ideal case. However, there may be some play in the joint, which leads to a nonzero angle [rotation in the lateral (y) direction] between the extension and the platform. The platform itself is attached to six legs via the leg-platform joints, which allow three rotational degrees of freedom (DoF). The legs are rigid and are linked to the base via the base-leg joints, which also allow three rotational DoF. However, the base-leg joints additionally allow one translational DoF per leg. The dislocation of one out of six base-leg joints is denoted as u and the six dislocations together are denoted as $\mathbf{u}$. The base is fixed to the inertial frame of reference. In

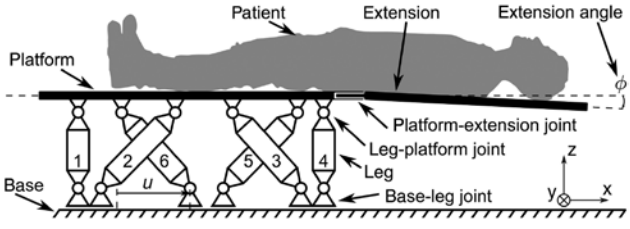

Figure 1: Schematic of the Protura with a patient.
The Protura allows the positioning in six degrees of freedom (DoF). The head and torso of the patient lie on the extension and the legs are positioned on the platform. The extension is removable via the platform-extension joint. The platform is connected to the legs via the rotational DoF leg-platform joints. The legs are rigid and connected to the base, which is fixed to the inertial frame of reference. The base-leg joints also allow rotational DoF, but additionally they each allow one translational DoF. The dislocation along this DoF is denoted as u. The platform-extension joint has some play resulting in a nonzero extension angle ϕ between the extension and the platform.

the coordinate system of the Protura, x represents the longitudinal direction, y the lateral direction, and z the vertical direction. The Protura allows the positioning of a patient in six DoF (three orthogonal translations and rotations).

The mechanics of the Protura operate similarly to a standard Stewart platform [4], where the legs consist of prismatic joints. The lengths of those legs can be set via electric motors independently of each other, resulting in defined positions and orientations of the platform. In contrast, the Protura's legs have fixed lengths, and the base-leg joints may move in one additional dimension. Each of them can be set independently, and each combination of base-leg joints' positions corresponds to a position and orientation of the platform. Therefore, first, the positions of the base-leg joints are computed for a given reference position and orientation of the platform. Then, the controller drives the actual base-leg joints to the computed reference positions. To the best of our knowledge, such kinematics have not yet been modeled before.

The Protura was modeled as depicted in Figure 2. The "Protura mechanics" represents the mechanical parts and the "internal controller" designates the controller of the Protura. This controller was considered given and nonmodifiable. The "internal controller" requires the desired position $\mathbf{t}_{ref}$, the orientation $\mathbf{q}_{ref}$ of the platform, and the current positions $\mathbf{u}$ of the base-leg joints as inputs. Its outputs are the forces $\mathbf{F}$ acting on the base-leg joints along the translational DoF. The "Protura mechanics" receives $\mathbf{F}$ as inputs, while the outputs are $\mathbf{u}$ and additionally the platform position $\mathbf{t}$ and orientation $\mathbf{q}$, as well as the extension angle ϕ. The electric motors were assumed to have no dynamics as well as no saturations and, therefore, were not explicitly modeled.

Protura mechanics

The subsystem "Protura mechanics" was modeled by a simplified system consisting of the platform, the extension, the base, and one leg. This approach and the derivation of the "Protura mechanics" equations of motions were taken from [4], but were adapted to the Protura.

Figure 3 shows the relevant points and vectors. O is the origin of the "Protura mechanics" and is fixed to the base, B_i is the location of the base-leg joint of leg i, and B_{i0} is the initial location of B_i. The leg's center of gravity (CG) is L_{iCG}. The geometrical center of the platform is T and the CG is T_{CG}. The leg-platform joint is J_i, the platform-extension joint is E and, finally, the CG of the extension is E_{CG}.

The positions of the points relative to the origin are described by vectors and rotations of the rigid bodies relative to the base

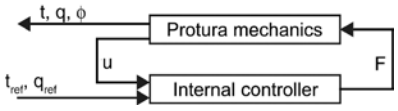

Figure 2: Signal flow diagram of the Protura, which is divided in two subsystems, the "Protura mechanics" and the "internal controller". The "Protura mechanics" subsystem is driven by the input forces $\mathbf{F}$ acting at the base-leg joints. Its outputs are the current position $\mathbf{t}$, orientation $\mathbf{q}$, the extension angle ϕ, and the base-leg joints positions $\mathbf{u}$. The "internal controller" subsystem's inputs consist of $\mathbf{u}$, the reference position $\mathbf{t}_{ref}$ and orientation $\mathbf{q}_{ref}$. Its outputs are the forces $\mathbf{F}$.

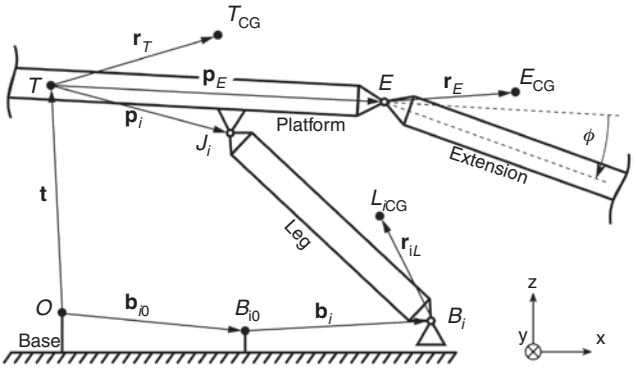

Figure 3: Representative sketch of the Protura to derive the model of the "Protura mechanics".
The capital letters represent geometrical points of the system. The lowercase bold letters represent vectors connecting the points. i, Leg number; O, origin of system; T, center of platform; B_i, base-leg joint position; B_{i0}, initial base-leg joint position; J_i leg-platform joint position; E, point on joint edge of extension; E_{CG}, center of gravity (CG) of extension; L_{iCG}, leg CG; T_{CG}, platform CG.

coordinate system (Figure 3). To know the positions of all points of the "Protura mechanics" only the vector $\mathbf{t}$, the platform's current rotation (orientation), and the extension angle ϕ are needed. The rotation of the platform is represented by quaternions $\mathbf{q}$, which are similar to complex numbers. Quaternions are widely used to describe rotations in three dimensions [15]. The variables $\mathbf{t}$, $\mathbf{q}$, and ϕ are the minimal coordinates of the "Protura mechanics" and were used to derive the kinematics which define the location of any point of the "Protura mechanics". The equations for the linear and angular momentum of the platform, the extension, and the legs are described in the supplementary material provided online. The final equation has the form of (1), which allowed the equations to be solved numerically.

$$\mathbf{M}(\mathbf{t},\mathbf{q},\phi)\cdot\begin{pmatrix}\ddot{\mathbf{t}}\\ \dot{\omega}_{IT}\\ \ddot{\phi}\end{pmatrix}=\mathbf{f}(\mathbf{t},\mathbf{q},\phi,\dot{\mathbf{t}},\omega_{IT},\dot{\phi},\mathbf{F}) \tag{1}$$

The left-hand side of (1) consists of $\mathbf{M}$, the mass matrix, multiplied with the second derivative of the minimal coordinates (accelerations). The entries of the mass matrix depend on the minimal coordinates. The right-hand side consists of the vector $\mathbf{f}$, whose entries are functions of the minimal coordinates ($\mathbf{t}$, $\mathbf{q}$, ϕ), the first derivative of the minimal coordinates ($\dot{\mathbf{t}}$, ω_{IT}, $\dot{\phi}$), and the input forces $\mathbf{F}$ given by the "internal controller".

Internal controller

The signal flow diagram of the "internal controller" is shown in Figure 4. The "reference conversion" computes $\mathbf{u}_{ref}$ from the reference input $\mathbf{t}_{ref}$ and $\mathbf{q}_{ref}$ using the kinematics of the "Protura mechanics". The "trajectory generator" limits the derivatives of its input signals, such that the input and output are identical as long as the derivatives of the inputs respect the given limits, which allows for taking into account the Protura's maximum speeds and accelerations. The method of limiting the derivatives of a signal is adopted from [1].

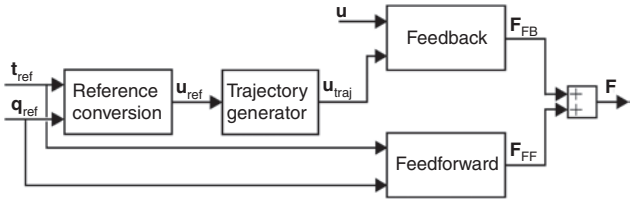

Figure 4: Signal flow diagram of the "internal controller".
The inputs are the references $\mathbf{t}_{ref}$, $\mathbf{q}_{ref}$, and the current base-leg positions $\mathbf{u}$. The output is $\mathbf{F}$, which is also the input to the mechanical system. The "reference conversion" converts the platform position to the positions $\mathbf{u}_{ref}$. The "trajectory generator" limits the derivatives of $\mathbf{u}_{ref}$. The "feedback" computes $\mathbf{F}_{FB}$ from the difference of $\mathbf{u}$ and $\mathbf{u}_{traj}$, while the "feedforward" computes $\mathbf{F}_{FF}$ from the reference input. The sum of $\mathbf{F}_{FB}$ and $\mathbf{F}_{FF}$ results in $\mathbf{F}$.

The $\mathbf{u}_{traj}$ signal is fed together with the actual base-leg joints positions $\mathbf{u}$ to the "feedback" controller, which consists of proportional-integral-differential (PID) controllers that work in parallel, thereby resulting in six PID controllers. The six PID controllers adjust the respective positions of the base-leg joints independently. The outputs of the "feedback" controllers are the forces $\mathbf{F}_{FB}$. In parallel to the "feedback" controller, there is the "feedforward" controller computing $\mathbf{F}_{FF}$. The "feedforward" controller uses the "Protura mechanics" equations with all the derivatives set to zero and solved for $\mathbf{F}$. These $\mathbf{F}$ are the forces needed to keep the "Protura mechanics" in steady state at the reference position $\mathbf{t}_{ref}$ and with the orientation $\mathbf{q}_{ref}$. The output of the "internal controller" $\mathbf{F}$ is the sum of $\mathbf{F}_{FB}$ and $\mathbf{F}_{FF}$.

Hardware setup

For the measurements on the Protura, one PC communicated with all the devices used in this study (Figure 5). The software used consisted of MATLAB/Simulink and Real Time Windows Target (The MathWorks Inc., Natick, MA, USA), which enabled the real-time execution of the calculations as well as the synchronization of all signals. The most important actuator was the Protura (CIVCO, Kalona IA, USA), to which the PC communicated via a serial interface. The other actuator, the Hexapod (Hexapod H840.5PD, Physik Instrumente GmbH & Co. KG, Karlsruhe/Palmbach, Germany), communicated in the same way and was used to mimic the respiratory motions of the patients. The sensors consisted of two laser triangulation systems (LTS) (optoNCDT 1302, Micro Epsilon Messtechnik GmbH & Co. KG, Ortenburg, Germany), which measured the position of a point on the Protura or the Hexapod. The specific setup of the sensors depended on the actual experiments described in the sections "Parameter estimation", "Parameter verification", and "Influence of extension". The sensors sent analog signals to the PC with an integrated data acquisition card (MF624, Humusoft, Prague, Czech Republic) that converted analog to digital signals. This converter worked with 14 bits, while the measuring range of the laser sensors was 50 mm, which resulted in a quantization of approximately 0.003 mm.

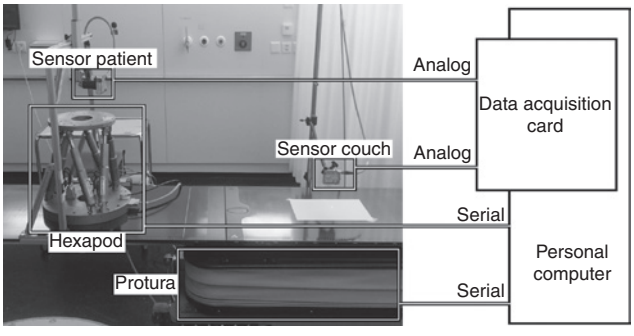

Figure 5: Hardware setup for experiments.
"Sensor patient" measures either the respiratory motion ("Hexapod") or the position of the Protura, while "sensor couch" measures the position of the Protura. If both sensors measure the Protura position, they measure different directions. The "data acquisition card" converts the analog signals to digital signals. The "Protura" and the "Hexapod" communicate with the "personal computer" (PC) via serial interfaces.

Parameter estimation

The known parameters included the geometrical parameters, such as the locations of the leg-platform joints, the lengths of the legs, as well as the inertias of the bodies of the Protura mechanics. However, there were unknown parameters, which had to be identified, namely, the maximum speeds, the maximum accelerations, the friction coefficients, and the parameters of the PID controllers. The unknown parameters concerning the extension were not identified, therefore, the experiments described in the following were carried out without the extension. But the influence of the extension on the rotational behavior of the Protura was considered in the section "Influence of extension".

For the identification of the unknown parameters, a sinusoidal chirp signal (linear increase of frequency from 0.01 Hz to 1 Hz in 200 s, amplitude of 10 mm) was used. The chirp signal was applied in the longitudinal direction (x chirp), the vertical direction (z chirp), and both directions simultaneously (xz chirp). The frequency range was chosen such that the typical breathing frequencies were included (0.27 Hz average, according to [19]).

The LTS sensors always measured the longitudinal (x) and vertical (z) position of the platform. In the case of xz chirp, the measurement was repeated with one sensor repositioned to measure the lateral (y) position.

In the first step, the speed and acceleration limits imposed by the trajectory generator were identified using the chirp signal measurements. The trajectory generator limits the speeds and accelerations of the positions of the base-leg joints rather than the platform position directly. But the known geometrical parameters and the kinematics of the Protura mechanics allowed the positions $\mathbf{u}$ to be computed from the measured platform position. Each position u was then fitted at each time step t_k with both a linear and a quadratic polynomial p over an interval Δt of 0.5 s, which yielded the speeds and the accelerations, respectively. The first derivative of the linear polynomial is the speed, while the second derivative of the quadratic polynomial is the acceleration. The peaks of the resulting sinusoidal signals yield the maximum values.

$$u(\tau)=p(\tau)+\text{error}(\tau), \quad t_k-\frac{1}{2}\Delta t<\tau\leq t_k+\frac{1}{2}\Delta t \tag{2}$$

Given the speed and acceleration limits of the trajectory generator, the friction coefficients and PID controller parameters were estimated

using the same chirp signals. The quality of the estimations were evaluated using Bode diagrams.

Parameter verification

The verification of the parameters identified was not carried out with chirp signals, but with data closer to actual tumor tracking. The following experiment was performed. The Hexapod was placed on the Protura platform and one LTS sensor measured the vertical motion of the Hexapod while being attached to the Protura platform. The motion of the Protura platform was measured by the other LTS sensor. Ten respiratory patterns were sent to the Hexapod. These patterns were previously acquired during a four-dimensional computer tomography scan using the respiratory patient monitoring system (RPM, Varian Medical Systems, Palo Alto, CA, USA). Based on a patient-specific correlation model, the one-dimensional external motion was converted to a three-dimensional internal motion. This motion was assumed to be the actual tumor motion and was compensated by the Protura in the longitudinal and the vertical directions but not in the lateral direction. The tumor sites consisted of lung, liver, and adrenal glands. The characteristics of these motion patterns, such as frequencies and amplitudes are listed in tables in the Supplement in Section 3. The time delay in the system was not compensated. The model was used to simulate the tumor tracking with the same respiratory patterns and correlation models. For both the model and the Protura the root mean square of the tracking error (e_{RMS}) was computed for ten different respiration cases.

Influence of extension

As mentioned above, these experiments were carried out without the extension. As the patient is placed mainly on the extension, its behavior is expected to have a great influence on the tracking error. Additionally, the motion of the extension relative to the platform is not known to the Protura. Therefore, we looked at the behavior of the angle ϕ between the platform and the extension. The experiment was set up as follows: First, the two LTS sensors were placed at one end of the Protura where they measured the vertical position of the Protura while it made a vertical step without load. The two LTS sensors were then shifted repeatedly a certain distance along the longitudinal direction of the Protura, while the measurement and the step were repeated after each shift. Figure 6 shows the resulting measurement positions. The measurement data was processed as follows: At each time sample of the measurements, two linear regressions were performed, with the first representing the platform and the second the extension.

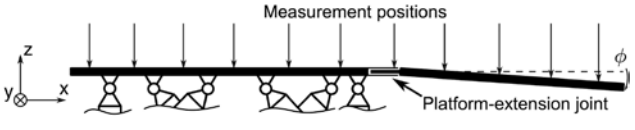

Figure 6: Measurement setup for examining the influence of the extension.
The vertical arrows point to the position measurement locations.

Results

Parameter estimation

Speed and acceleration limitations

The mean values of the maximum velocities of the platform show larger variations than those of the base-leg joints (Table 1). The highest accelerations were reached with the z chirp for both the platform and the base-leg joints. Furthermore, results of simulations with the model were acquired with a speed limit of 20.09 mm/s and an acceleration limit of 72.93 mm/s^2.

Input-output behavior with estimated parameters

The Protura was able to follow the amplitude of the input signal in the longitudinal direction up to 0.40 Hz, but it lagged behind as the phase decreased from -4.31° at 0.10 Hz to -22.41° at 0.35 Hz (Figure 7). The magnitude of the measurement peaks at 0.37 Hz reaching 1.22 dB. The magnitudes

Table 1: Absolute values of maximum velocities and accelerations of the platform and the base-leg joints for x chirp, z chirp, and xz chirp (mean±standard deviation).

	x chirp	z chirp	xz chirp
Platform			
Speed (mm/s)	20.21±1.13	18.62±1.09	14.77±0.37
Acceleration (mm/s^2)	55.18±3.78	68.94±5.53	45.06±5.16
Base-leg joints			
Speed (mm/s)	20.09±1.28	19.37±1.29	18.79±0.29
Acceleration (mm/s^2)	56.18±4.78	72.93±6.16	55.80±4.13

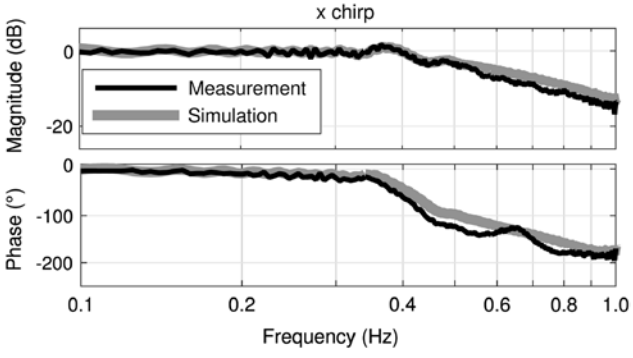

Figure 7: Bode diagram of the Protura (Measurement) and the model (Simulation), which followed an x chirp.
The input is the chirp signal and the output is the actual longitudinal position of the platform.

of the model and of the measurement matched over the entire frequency range. Except for the frequency range between 0.44 Hz and 0.73 Hz, the phases also matched.

The Protura managed to follow the magnitude of signals in the vertical direction with up to 0.38 Hz (Figure 8), but also here the phase showed a decrease from -6.65° at 0.10 Hz to -13.70° at 0.33 Hz. The match in magnitude between the model and the Protura was accurate up to 0.40 Hz and above 0.80 Hz. The phases match up to 0.37 Hz and diverge as the frequency increases.

Figure 9 shows the tracking behavior of the Protura in the vertical direction, when it followed a chirp signal in the vertical as well as in the longitudinal direction. The magnitude was zero up to 0.23 Hz and decreased as the frequency increased. The phase also showed a decrease from -7.05° at 0.10 Hz to -21.64° at 0.21 Hz. In this case, the magnitudes of the model and of the Protura matched at frequencies of up to 0.35 Hz and at frequencies above 0.86 Hz. The phases matched up to 0.80 Hz. The tracking behavior was similar in the longitudinal direction.

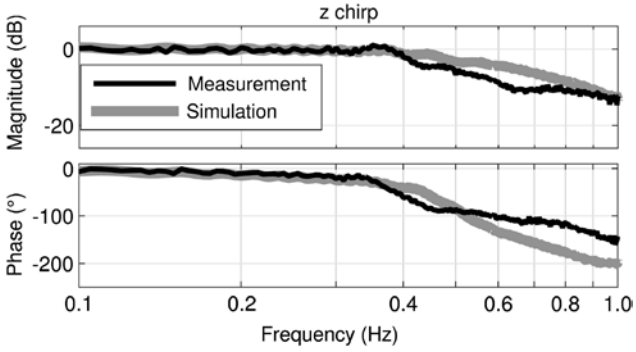

Figure 8: Bode diagram of the Protura (Measurement) and the model (Simulation), which followed a z chirp.
The input is the chirp signal and the output is the actual vertical position of the platform.

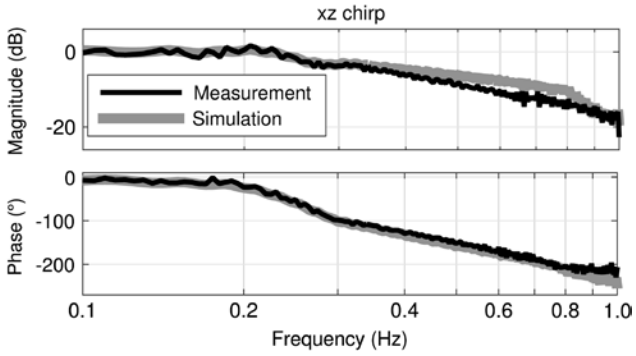

Figure 9: Bode diagram of the Protura (Measurement) and the model (Simulation), which followed a xz chirp signal.
The input is the chirp signal, while the output is the actual vertical position of the platform.

In the case of simultaneous vertical and longitudinal motions, the Protura also exhibited a lateral motion even when the corresponding reference value was set to zero. In Figure 10, the magnitude of the Bode diagram shows the transfer function of the vertical reference input and the lateral position output of the Protura and of the model. The Protura had a peak magnitude of about -9.25 dB at a frequency of 0.36 Hz. The magnitude of the model peaked at -13.41 dB at 0.32 Hz and thus was smaller than that of the Protura at frequencies above 0.28 Hz, but the magnitudes matched at frequencies below this value.

Parameter verification

The root mean square of the tracking error (e_{RMS}) was computed for respiration measurements and correlation models of ten different patients (Figure 11). The white bars show the error without using tracking. The black bars show the measured tracking errors, while the gray bars represent the tracking errors of the simulation. Couch tracking always reduced the tracking error, but with variations over the respiration patterns of the patients. The median reduction of the measured tracking errors was 69% with a standard deviation of 17%, while the respective values for the model were 80% and 17%, respectively. The Pearson correlation coefficient between the reductions of the Protura and the model was 0.99.

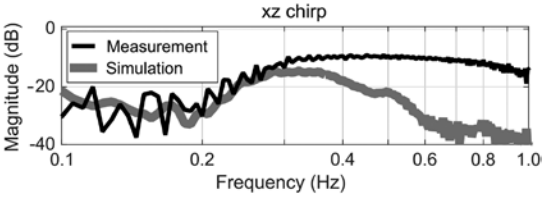

Figure 10: Bode diagram of the Protura (Measurement) and the model (Simulation), with the vertical longitudinal reference as the input and the unintended lateral motion as the output during an xz chirp.

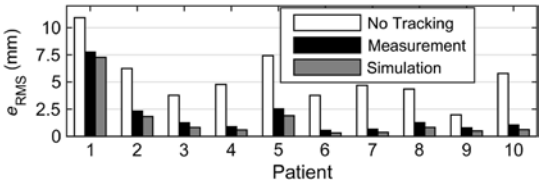

Figure 11: Comparison of tumor-tracking performances simulated with the Protura (Measurement) and the model (Simulation) for ten different patients.
Each patient had a specific respiratory behavior and tumor motion. "No tracking" represents a static couch. The variable e_{RMS} is the root mean square of the tracking error.

Influence of extension

The profile of the Protura, as seen from the lateral direction, is shown in Figure 12 during a vertical step of 20 mm. The line segments on the left side represent the platform and those on the right represent the extension, corresponding to the schematic of Figure 1. Each pair is a side-view snapshot of the Protura with the corresponding times marked on the left. The step motion started at time 2 s and took about 1.5 s to complete.

The platform and the extension were horizontal before the step motion and afterwards. However, during the step there was a height difference of approximately 2 mm between the far left end of the platform and the far right end of the extension. Figure 13 shows the corresponding tilt angles around the lateral axis of both the platform and the extension. The angles were nonzero during the step. Additionally, in the first half-second of the step, the tilt angles of the platform and the extension differed.

Discussion

In this study the tracking behavior of the Protura was modeled and its performance was tested. For all respiration trajectories tested the tumor motion relative to the radiation beam was reduced by a median of 69% (Figure 11). However, in some circumstances there was an unintended lateral motion, especially at increased frequencies. The extension caused nonnegligible rotational motion around the lateral axis of the Protura, even though the corresponding reference was zero. The model represents the Protura well, which allows experiments on the Protura to be replaced by tests on the model.

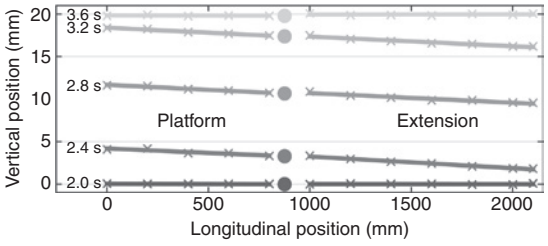

Figure 12: The sideways profile of the platform (left line segments) and the extension (right line segments) of the Protura during a measured vertical step of 20 mm shown at several time instances (marked on the left).
The crosses show the measured values, the lines the linear regression fits and the dots the location of the platform-extension joint.

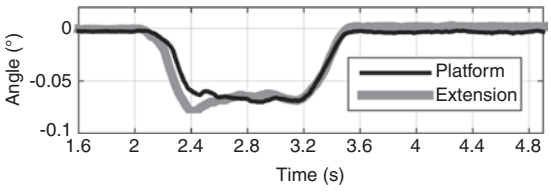

Figure 13: The tilt angle (lateral rotation) of the platform and the extension during a vertical step of 20 mm of the Protura.

In our earlier work, we reported the maximum speed of the Protura to be 16 mm/s [16], which corresponds to the platform speed. The Protura is actually limited in the speed of the base-leg joints, so the maximum speed of the platform depends only on the type of motion which the platform has to execute. The limit of 16 mm/s is valid for a motion in general directions, but it does not hold true for a motion in only one, e.g. the vertical direction. In this case, the speed of the Protura may reach 20 mm/s. Its maximum speed lies between the maximum speeds of the other treatment couches: the HexaPOD is stated to reach 8 mm/s [11], while maximum speed of the ELEKTA Precise Table is specified to reach 40 mm/s [9]. No information is publicly available on the maximum accelerations of those two. D'Souza et al. [7] developed specifications of an ideal treatment couch for tumor tracking. Such a couch should reach speeds of 162 mm/s and accelerations of 887 mm/s. Both specifications are an order of magnitude larger than the values achieved by the Protura. These specifications, however, are very conservative and the majority of tumor speeds do not reach such high values, but are below 16 mm/s [20].

To the best of our knowledge, the Protura has not yet been modeled. The most similar system that was modeled is the HexaPOD [11]. A blackbox model was derived, which required the identification of parameters. Chirp signals were also employed, and in the case of vertical motion, the HexaPOD could fully track the chirp signal up to about 0.3 Hz. The Protura reached only slightly higher values for pure longitudinal or vertical motion, even though the maximum speed of Protura was twice as high. This can be explained by the fact that the amplitudes of the chirp signals were different. An amplitude of 10 mm was used, while for the HexaPOD it was only 5 mm. The maximum speed of the chirp signal of the HexaPOD amounted to only one-half of those of the Protura, which corresponded with the maximum speed of the treatment couches. Additionally, there may be differences between the HexaPOD and the Protura in the phase lag. The HexaPOD was also modeled in [3] using an approach that included the underlying mechanics. However, the parameters of the HexaPOD were considered to be known and

no identification and verification of the model's parameters were carried out.

The Bode plots (Figures 7–10) show a good match between the Protura and the model for frequencies of up to 0.3 Hz, although the unintended lateral motion limits the model. Therefore, the model allows the behavior of the Protura to be predicted accurately for respiratory motion tracking with frequencies of up to 0.3 Hz.

The lateral motion can be explained by the particular setup of the Protura mechanics. Legs 1 and 4 (Figure 1), at the short ends of the platform, exert lateral forces on the platform. During a vertical motion of the platform, the base-leg joints of these two legs move to different locations, which results in nonzero errors. The PID controllers translate the nonzero errors into nonzero forces in the lateral direction. Thus, there are lateral forces acting on the platform even though none are needed. The faster the vertical motion was, the larger the forces were acting in the lateral direction and the more motion occurred in the lateral direction. The discrepancy observed may be due to differences between the parameters of the PID controllers of the model and the Protura.

Figure 11 shows that the model accurately predicted the tumor-tracking performance of the Protura, although with a tendency to decreased tracking errors. This difference in tracking errors can be corrected by a linear function as indicated by the correlation of 0.99. It was observed that tumor tracking always decreased the tumor motion relative to the beam. The root mean square of the tracking error values varied between 0.31 mm and 7.76 mm, corresponding to reductions by 86% and 29%, respectively.

The tracking errors reported in other works were mostly smaller than the results shown in Figure 11. For example in [9], the root mean squares of the tracking errors of the ELEKTA Precise Table were reported to be between 0.81 mm and 1.03 mm, corresponding to motion reductions by about 80%. In [10], the values reported for the HexaPOD were between 0.03 mm and 1.62 mm. Nevertheless, the results of seven tracking cases of our study were comparable to those from the literature, with only one large outlier (patient 1). The Protura was evaluated in an earlier study by our group [16], and there the median tumor motion reduction was reported to be about 90%, which is higher than the 69% achieved in this work. However, only vertical tracking was considered in [16], which allows a higher performance, as shown in Figures 8 and 9. Tumor-tracking systems based on different techniques were also considered in the literature. In [12], a reduction of up to 82% (reduction factor of 5.7) was achieved with the CyberKnife System (Accuray Inc., Sunnyvale CA, USA), when treating lung cancer patients with tumor motion amplitudes of up to 15 mm in cranial-caudal and 10 mm in anterior-posterior direction. In [5], a gimbal-based system was used for tumor tracking. A sinusoidal motion (20 mm amplitude) was tracked, and a motion reduction of at least 85% was achieved. In [13], a multi-leaf collimator was used for tumor tracking, and motion reductions of up to 83% were accomplished when tracking a sinusoidal motion with 20 mm amplitude. These results of alternative techniques show reductions on the same order of magnitude as the Protura's reductions. As the results varied depending on the current respiration patterns, standardized respiration trajectories would be required to yield valid comparisons. The tumor motion patterns used in this work varied in their superior-inferior amplitudes between 4.9 mm and 24.8 mm, and in anterior-posterior direction between 1.2 mm and 14.6 mm, respectively. The frequencies varied between 0.14 Hz and 0.4 Hz.

Figures 12 and 13 show that the rotations of the platform and the extension need to be considered as well. Even without a load, the platform and the extension showed a tilt angle around the lateral axis. This fact greatly affects the position of the tumor relative to the beam because the patient's torso is placed on the extension as depicted in Figure 1. While the "internal controller" could keep the rotation of the platform at the reference value in the steady state case, it was unable to do so in the transient case. Additionally, because the extension is flexible, any loads can bend it, which was considered in [9]. The unintended rotation and the flexibility of the extension emphasize the need to consider the influence of the extension in tumor tracking.

Preliminary tests showed very small influence of the patient's weight on the performance of the Protura and were therefore neglected in the measurements, as were the three-dimensional rotations of the platform. The time delay of the Protura was not explicitly considered, but was implicitly included in the results of the chirp signal measurements.

The reduction of the tumor motion is expected to reduce the radiation dose to the healthy tissue. Figure 11 shows that tumor tracking reduced the amplitude of the tumor motion by 69% (median) compared to "no tracking". A reduction of the respiratory amplitude of 50% leads to a reduction in the mean lung dose (surrounding healthy tissue) of about 30% [8]. This can be expected for treatment couch tracking with the Protura and may lead to reduced side effects such as pneumonitis.

Conclusion

Although the Protura is only designed for pre-treatment positioning of the patients, it can be used to compensate for tumor motion below the speed limit of the Protura. The compensation for faster tumor motion is challenging, and the resulting reduction of tracking errors depends very much on the respiration pattern. The unintended lateral motion becomes relevant at increased frequencies. To avoid such unwanted motions, an "internal controller" compensating for lateral motion may be required. The extension introduces additional dynamics, which have to be taken into account when the Protura is used for tumor tracking.

The model represents the Protura well and can be used as a substitute for the Protura to conduct initial tests of algorithms such as prediction filters that are used for tumor tracking.

Nomenclature

B	base-leg joint location
B_0	initial base-leg joint location
CG	center of gravity
DoF	degree(s) of freedom
E	platform-extension joint
E_{CG}	center of gravity of extension
$\mathbf{F}$	input forces of mechanical system
J	leg-platform joint location
L_{CG}	center of gravity of leg
$\mathbf{M}$	generic mass matrix of (1)
O	inertial origin of system
PID	proportional-integral-differential
T	geometrical center of platform of treatment couch
T_{CG}	center of gravity of platform of treatment couch
e_{RMS}	root mean squared error
$\mathbf{t}$	vector from origin to center of platform
$\mathbf{t}_{ref}$	reference platform position
$\mathbf{q}$	quaternion vector for rotation of platform
$\mathbf{q}_{ref}$	reference quaternion for rotation of platform
u	one base-leg position (a component of $\mathbf{u}$)
$\mathbf{u}$	base-leg positions
$\mathbf{u}_{ref}$	reference base-leg positions
$\mathbf{u}_{traj}$	derivative limited reference base-leg positions
ϕ	angle of extension relative to platform
ω_{IT}	rotational velocity of platform

Acknowledgments: This work was supported by the Swiss National Science Foundation (SNSF) through "Development of prediction models for liver, lung, and breast tumors and implementation and verification of prediction filters for advanced couch tracking in a clinical environment", Grant No. CR32I3_153491.

References

[1] Biagiotti L, Zanasi R. Time-optimal regulation of a chain of integrators with saturated input and internal variables: an application to trajectory planning. In: 8th IFAC Symposium on Nonlinear Control Systems. 2010; 1278–1283.
[2] Buzurovic I, Huang K, Yu Y, Podder TK. A robotic approach to 4D real-time tumor tracking for radiotherapy. Phys Med Biol 2011; 56: 1299.
[3] Buzurovic I, Podder T, Huang K, Yu Y. Tumor motion prediction and tracking in adaptive radiotherapy. In: BioInformatics and BioEngineering (BIBE), 2010 IEEE International Conference on. 2010; 273–278.
[4] Dasgupta B, Mruthyunjaya T. Closed-form dynamic equations of the general stewart platform through the Newton-Euler approach. Mech Mach Theory 1998; 33: 993–1012.
[5] Depuydt T, Verellen D, Haas O, et al. Geometric accuracy of a novel gimbals based radiation therapy tumor tracking system. Radiother Oncol 2011; 98: 365–372.
[6] Dieterich S, Suh Y. Tumor motion ranges due to respiration and respiratory motion characteristics. In: Uschel HC, Kresl JJ, Luketic JD, Papiez L, Timmerman RD, Schulz RA, editors. Treating tumors that move with respiration. Berlin, Heidelberg: Springer 2007: 3–13.
[7] D'Souza WD, McAvoy TJ. An analysis of the treatment couch and control system dynamics for respiration-induced motion compensation. Med Phys 2006; 33: 4701–4709.
[8] Guckenberger M, Kavanagh A, Webb S, Brada M. A novel respiratory motion compensation strategy combining gated beam delivery and mean target position concept – a compromise between small safety margins and long duty cycles. Radiother Oncol 2011; 98: 317–322.
[9] Haas OC, Skworcow P, Paluszczyszyn D, Sahih A, Ruta M, Mills JA. Couch-based motion compensation: modelling, simulation and real-time experiments. Phys Med Biol 2012; 57: 5787.
[10] Herrmann C, Ma L, Wilbert J, Baier K, Schilling K. Control of a HexaPOD treatment couch for robot-assisted radiotherapy. Biomed Tech (Berl) 2012; 57: 333–351.
[11] Herrmann C, Schilling K, Ma L. Modeling a HexaPOD for tumor motion compensation in robot assisted radiotherapy. In: Proceedings of the Joint Conference of the 41st International Symposium on Robotics and the 6th German Conference on Robotics. Munich, Germany: June 2010.
[12] Hoogeman M, Prvost JB, Nuyttens J, Pöll J, Levendag P, Heijmen B. Clinical accuracy of the respiratory tumor tracking system of the cyberknife: Assessment by analysis of log files. Int J Radiat Oncol Biol Phys 2009; 74: 297–303.
[13] Keall PJ, Cattell H, Pokhrel D, et al. Geometric accuracy of a real-time target tracking system with dynamic multileaf collimator tracking system. Int J Radiat Oncol Biol Phys 2006; 65: 1579–1584.
[14] Keall PJ, Mageras GS, Balter JM, et al. The management of respiratory motion in radiation oncology report of AAPM Task Group 76. Med Phys 2006; 33: 3874–3900.
[15] Kuipers JB. Quaternions and rotation sequences, vol. 66. Princeton: Princeton University Press 1999.
[16] Lang S, Zeimetz J, Ochsner G, Schmid Daners M, Riesterer O, Klöck S. Development and evaluation of a prototype tracking system using the treatment couch. Med Phys 2014; 41: 021720.

[17] Quirk S, Becker N, Smith W. External respiratory motion analysis and statistics for patients and volunteers. J Appl Clin Med Phys 2013; 14: 90–101.
[18] Rohlfing T, Maurer Jr CR, ODell WG, Zhong J. Modeling liver motion and deformation during the respiratory cycle using intensity-based nonrigid registration of gated MR images. Med Phys 2004; 31: 427–432.
[19] Seppenwoolde Y, Shirato H, Kitamura K, et al. Precise and real-time measurement of 3D tumor motion in lung due to breathing and heartbeat, measured during radiotherapy. Int J Radiat Oncol Biol Phys 2002; 53: 822–834.
[20] Shirato H, Suzuki K, Sharp GC, et al. Speed and amplitude of lung tumor motion precisely detected in four-dimensional setup and in real-time tumor-tracking radiotherapy. Int J Radiat Oncol Biol Phys 2006; 64: 1229–1236.

Supplemental Material: The online version of this article (DOI: 10.1515/bmt-2015-0187) offers supplementary material, available to authorized users.